Facile Melting-Crystallization Synthesis of Cs(2)Na(x)Ag(1-x)InCl(6): Bi Double Perovskites for White Light-Emitting Diodes

Xiaoxi Li, Weiwei Li, Mengling Xia, Chao Liu, Neng Li, Zuhao Shi, Yinsheng Xu, Xianghua Zhang

▶ **To cite this version:**

Xiaoxi Li, Weiwei Li, Mengling Xia, Chao Liu, Neng Li, et al.. Facile Melting-Crystallization Synthesis of Cs(2)Na(x)Ag(1-x)InCl(6): Bi Double Perovskites for White Light-Emitting Diodes. Inorganic Chemistry, 2022, 61 (12), pp.5040-5047. 10.1021/acs.inorgchem.1c03996 . hal-03632025

HAL Id: hal-03632025
https://hal.science/hal-03632025v1

Submitted on 15 Jun 2023

HAL is a multi-disciplinary open access archive for the deposit and dissemination of scientific research documents, whether they are published or not. The documents may come from teaching and research institutions in France or abroad, or from public or private research centers.

L'archive ouverte pluridisciplinaire **HAL**, est destinée au dépôt et à la diffusion de documents scientifiques de niveau recherche, publiés ou non, émanant des établissements d'enseignement et de recherche français ou étrangers, des laboratoires publics ou privés.

Facile melting-crystallization synthesis of $Cs_2Na_xAg_{1-x}InCl_6$: Bi double perovskites for WLEDs

Xiaoxi Li[1], *Weiwei Li*[2], *Mengling Xia*[3], *Chao Liu*[1], *Neng Li*[1], *Zuhao Shi*[1], *Yinsheng Xu*[1,*], *Xianghua Zhang*[1,4,*]

[1] State Key Laboratory of Silicate Materials for Architectures, Wuhan University of Technology, Wuhan 430070, China

[2] State Key Laboratory of Advanced Technology for Materials Synthesis and Processing, Wuhan University of Technology, Wuhan 430070, China

[3] Wuhan National Laboratory for Optoelectronics (WNLO), Huazhong University of Science and Technology (HUST), Wuhan, Hubei 430074, China.

[4] ISCR (Institut Des Sciences Chimiques de Rennes) - UMR 6226, CNRS, Univ Rennes, 35000 Rennes, France

Keywords: double perovskite, WLED, melting-crystallization, STE

Abstract

Lead-free double perovskites (DPs) have outstanding luminescent properties, which makes them excellent candidates for wide uses in optoelectronics. Herein, a solvent-free melting-crystallization technique, which can produce kilogram-scale DP microcrystals (DP-MCs) in one batch, is invented to synthesize the $Cs_2Na_xAg_{1-x}InCl_6$: Bi (x=0, 0.2, 0.4, 0.6, 0.8 and 1) DP-MCs. The structure and composition analysis confirmed the products are pure $Cs_2Na_xAg_{1-x}InCl_6$ DP-MCs. Affecting by Jahn-Teller distortion of $AgCl_6$ octahedra, self-trapped excitons appear in the excited state, resulting in the broadband emission (400-850 nm) of $Cs_2Ag_{1-x}Na_xInCl_6$: Bi DP-MCs. The enhancement of the photoluminescence quantum yield (PLQY) can be realized by introducing Na^+ to break parity-forbidden transition in the $Cs_2AgInCl_6$ DP. Optimized $Cs_2Na_{0.4}Ag_{0.6}InCl_6$: Bi DP-MCs phosphors combined with commercial blue and green phosphors were coated on UV chips (365 nm) to fabricate White light-emitting diodes (WLEDs) from warm white (2930 K) to cold white (6957 K). An ultra-high color rendering index of 97.1 and a CCT of 5548 K as well as Commission Internationale de l´Eclairage color coordinates of (0.331, 0.339) have been demonstrated. This kilogram-scale synthesis technique could stimulate the industrial development of WLEDs for general lighting based on DP-MCs phosphors.

Introduction

WLEDs, which have the characteristics of long lifetime and low power consumption,[1-3] have received unprecedented attention from the entire community and are supposed to play a key role in future lighting. Many works so far have been focused on the synthesis of rare earth (RE) doped

phosphors with great progress. [4-6] However, RE have generally narrow emission peaks, with a full width at half maximum (FWHM) typically in the range of 20-60 nm,[7, 8] making it impossible to achieve high color rendering index (CRI). In addition, the scarcity of RE is also an important issue for application development. It remains challenging to find an alternative to RE doped phosphors.

Lead-free double perovskites (DPs) have received widespread attention due to their high absorption coefficient and high charge-carrier mobility.[9-12] Among these DPs, $Cs_2AgInCl_6$ has been intensively investigated because of its excellent moisture and light/heat stability as well as a direct bandgap of 3.3 eV.[13-15] Tang *et al*. synthesized $Cs_2AgInCl_6$ using the hydrothermal method and successfully broke its parity-forbidden transition by introducing Na^+, achieving a broadband warm white emission with photoluminescence quantum yield (PLQY) up to ~86%.[16] Xia's group demonstrated a hot-injection synthesis of $Cs_2AgInCl_6$: Bi nanocrystals, which presented typical self-trapped excitons (STEs) broad emission with 11.4% PLQY.[17] Bi element could serve as the surface deactivator to promote the radiative localization, therefore adjusting the band gap. Nevertheless, acids and other organic solvents were employed through the reaction, which would cause environmental pollution. The low solubility of reactants and the finite volume of the reaction vessel limit large-scale production. Moreover, the autoclave is dangerous at high pressure. Recently, Zhao *et al*. implemented a traditional high temperature solid-state reaction to synthesize $Cs_2AgInCl_6$: Cr^{3+} powder.[18] As well known, the solid-state reaction is a general technique to produce phosphors but requires that all reactants are fine powder and well mixed to make sure homogenization reaction. To produce large-scale inorganic perovskite phosphors, a low-cost, environmentally friendly, and high yield approach is needed.

In this work, a solvent-free melting-crystallization technique was invented to fabricate kilogram-scale $Cs_2Na_xAg_{1-x}InCl_6$: Bi DP-MCs. The formation energy of DP-MCs was calculated to confirm

that the reaction could take place in vacuum conditions. Crystal structure and morphology of the DP-MCs were investigated by XRD, Raman spectra, TEM, and SEM. The prepared $Cs_2Na_xAg_{1-x}InCl_6$: Bi DP-MCs exhibit a warm light broadband emission (400-850 nm) and high quantum efficiency up to 73.3, allowing us to fabricate WLED with commercial blue and green phosphors to get adjustable correlated color temperature (CCT). By coating mixed phosphors with silicone on 365 nm UV-LED chips, WLED with Commission Internationale de l´Eclairage (CIE) color coordinates of (0.331, 0.339) and a high CRI of 97.1 was realized.

Experimental details

Raw materials

Cesium chloride (CsCl, 99.9%), sodium chloride (NaCl, 99.9%), silver (I) chloride (AgCl, 99.9%), indium (III) chloride ($InCl_3$, 99.9%), and bismuth (III) trichloride ($BiCl_3$, 99.9%) were from Aladdin Biochemical Technology Co., Ltd. All the chemicals were used without further purification.

Synthesis

$Cs_2Na_xAg_{1-x}InCl_6$: Bi (with x=0, 0.2, 0.4, 0.6, 0.8 and 1) were synthesized by using melting-crystallization method. CsCl, NaCl, AgCl, and $InCl_3$ powders with a total weight of 100 g were weighed according to the composition and ground with an agate mortar in an argon-filled glove box, with 0.005 mol of $BiCl_3$ in addition. Then the mixture was sealed in a vacuum pumped silica tube (~5×10^{-5} Pa) to avoid evaporation and oxidation. The closed space ensures the following reaction at a high temperature.

$$2CsCl + InCl_3 + AgCl\ (NaCl) \rightarrow Cs_2InAg\ (Na)Cl_6 \quad (1)$$

To ensure a full reaction, the mixture was melted at 600 °C for 2 hours in a rocking furnace. Then the melting was slowly cooled to room temperature. The microcrystals were formed during the cooling process. The agglomeration was then ground into fine powders for subsequent characterization.

Characterization

The powder X-ray diffraction (XRD) patterns were collected on a Bruker D8 ADVANCE equipped with a Cu Kα (0.1541 nm) radiation source. The optical absorption spectrum of the powder was measured with a Shimadzu UV-3600 spectrophotometer at RT. The fluorescence spectra, PL decay curves, and PLQYs were obtained by using a fluorescence spectrophotometer (Edinburgh Instruments, FLS1000) equipped with a continuous 450 W xenon lamp as the excitation source. For measuring the temperature-dependent PL and fluorescence lifetime, the spectrofluorometer was equipped with a cryostat (Sumitomo HC-4E) to provide a continuous temperature variation from 30 K to 325 K. X-ray photoelectron spectroscopy (XPS) was measured with an ESCALAB 250 Xi spectrometer. Scanning electron microscopy (SEM) and energy dispersive X-ray spectroscopy (EDS) analyses were performed by using a JEOL JSM-7500F SEM equipped with a cold field-emission gun, operating at 15 kV acceleration voltage. High-resolution transmission electron microscopy (HRTEM) was carried out on a JEOL JEM-2100F electron microscope operating at 200 kV. Raman spectra were recorded using laser confocal micro-Raman Spectroscopy (LabRAM HR Evolution) with a 460 nm laser. No laser-induced degradation was observed.

Fabrication of WLED devices

WLED devices with GaN-based UV-LED chips (1 W output, 365 nm peak emission) were fabricated. The $Cs_2Ag_{0.6}Na_{0.4}InCl_6$: Bi microcrystals were ball-milled into a fine powder, mixed

with different ratios of commercial blue ($BaMgAl_{10}O_{17}$: Eu) and green ($(Sr, Ba)_2SiO_4$: Eu) phosphors, specific ratios of the three phosphors are illustrated in Table S4 (**Supporting Information**). Then uniformly dispersed into silicone and then coated on the UV-LED chips to form LEDs. The LED chips were driven by a Keithley 2400 source meter, and the emission spectra and intensity were recorded by the Everfine ATA-500 photoelectric analysis system. The temporal stability of the devices was monitored.

Theoretical Calculations

All total formation energy calculations were obtained from density functional theory (DFT) calculations,[19] as implemented in the DS-PAW program. The generalized gradient approximation (GGA) of the Perdew, Burke, and Ernzerhof (PBE) functional was used for the exchange correlation. For the structural optimization, a Γ-centered k-point grid of 4 × 4 × 5 for $Cs_2Na_xAg_{1-x}InCl_6$: Bi was applied to obtain the unstrained configuration and the plane wave cut offs of 80 and 400 Ry, as described above.

Results and discussion

As highly ionic compounds, DPs are usually dissolved and prepared in polar solvents[20] which may cause solvent pollution. As illustrated in **Figure 1a,** all the raw materials were mixed and heated to 600 °C for a melting reaction then cooled down slowly to room temperature. Using the solvent-free melting-quenching technique to synthesize the Bi doped $Cs_2Ag_{0.4}Na_{0.6}InCl_6$ DP-MCs, not only avoids the use of solvent but also enables rapid and convenient preparation of kilogram scale products. As demonstrated in **Table S1** (**Supporting Information**), the formation energy of $Cs_2AgInCl_6$ DP is -985.46 meV/unit, which is the lowest among all the compositions. With Na^+ introduction into the $Cs_2AgInCl_6$ lattice, the formation energy gradually increases to -716.03 meV/unit, implying that Na^+ is more difficult to be incorporated. However, this composition can

still be easily formed in a closed vacuum condition. The as-prepared product shows little yellowish white color under visible light and emits bright white fluorescence under 365 nm UV excitation (**Figure 1b**).

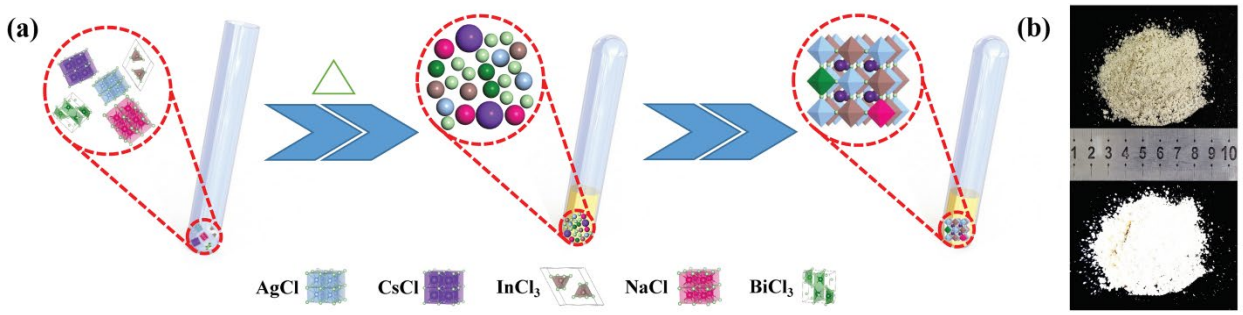

Figure 1. (a) Schematic diagram of the melting-crystallization synthesis for double perovskite microcrystals. (b) Photographs of the $Cs_2Ag_{0.4}Na_{0.6}InCl_6$: Bi powder under visible light (top) and UV illumination (bottom).

It was demonstrated in a number of studies that the $Cs_2AgInCl_6$ has a cubic structure with $Fm\bar{3}m$ space group,[21, 22] which agrees well with the TEM result shown in **Figure 2a**. As demonstrated in **Figure 2b**, the DP-MCs have distinguishable lattice fringes with a spacing of 0.3778 nm and 0.2667 nm, corresponding to the g_{220} and g_{400} lattice planes of the $Cs_2AgInCl_6$, respectively. This is consistent with the observation from the low dose selected area electron diffraction pattern in **Figure 2c**. Differential thermal analysis (DTA, **Figure S1**, **Supporting Information**) results revealed a decomposition temperature of about 575 °C, indicating that the almost defect-free lattice and the all-inorganic components can act together to resist thermal stress.[16] The XRD results of the compound show that $Cs_2Na_xAg_{1-x}InCl_6$: Bi DP-MCs have a similar face-centered cubic structure to $Cs_2NaInCl_6$ and $Cs_2AgInCl_6$, which matched well with the $Fm\bar{3}m$ space group (**Figure 2d**). As reported by Li *et al.*,[23] the exposed crystal facet of $Cs_2AgInCl_6$ single crystals can

be seen assigned to (111) as shown in **Figure S2 c-d** (marked in red circles). Notably, the intensity of the (111) peak (at 2θ=14.3º), which can be attributed to the ordering arrangement of B (=Na/Ag) and B' (=In) in halides double perovskites ($Cs_2B(I)B'(III)X_6$), is positively correlated with the content of Na^+. In our case, as the content of Na^+ increases, the intensity of the (111) peak also increases, indicating the antisite defects are negligible.[16] The peaks located at 2θ=23.56º and 2θ=33.67º represent the (220) and (400) planes, respectively, in agreement with both HRTEM and the corresponding Fast Fourier transform (FFT) analysis.[24, 25]

SEM images and EDS were also used to investigate the morphology and element distribution of the $Cs_2Ag_{0.4}Na_{0.6}InCl_6$: Bi DP-MCs. The magnified SEM images of the microcrystals show that it has a typical face centered cubic crystal characteristics and truncated octahedron (**Figure S2**, **Supporting Information**). To evaluate the composition uniformity of $Cs_2Ag_{0.4}Na_{0.6}InCl_6$: Bi DP-MCs, the EDS elemental mapping of a representative particle was studied (**Figure 2e and Figure S3, Supporting Information**). By analyzing the elements of Cs, Ag, In, Cl, and Na, it is found that they are all uniformly distributed in the crystal grain. Meanwhile, EDS data show that the molar ratio of Cs, Ag, Na, In, and Cl is 2.3 : 0.39 : 0.57 : 1.0 : 6.0, which is slightly different from the nominal composition (**Table S2, Supporting Information**). The doping concentration of Bi^{3+} was lower than the detection limit of EDS.

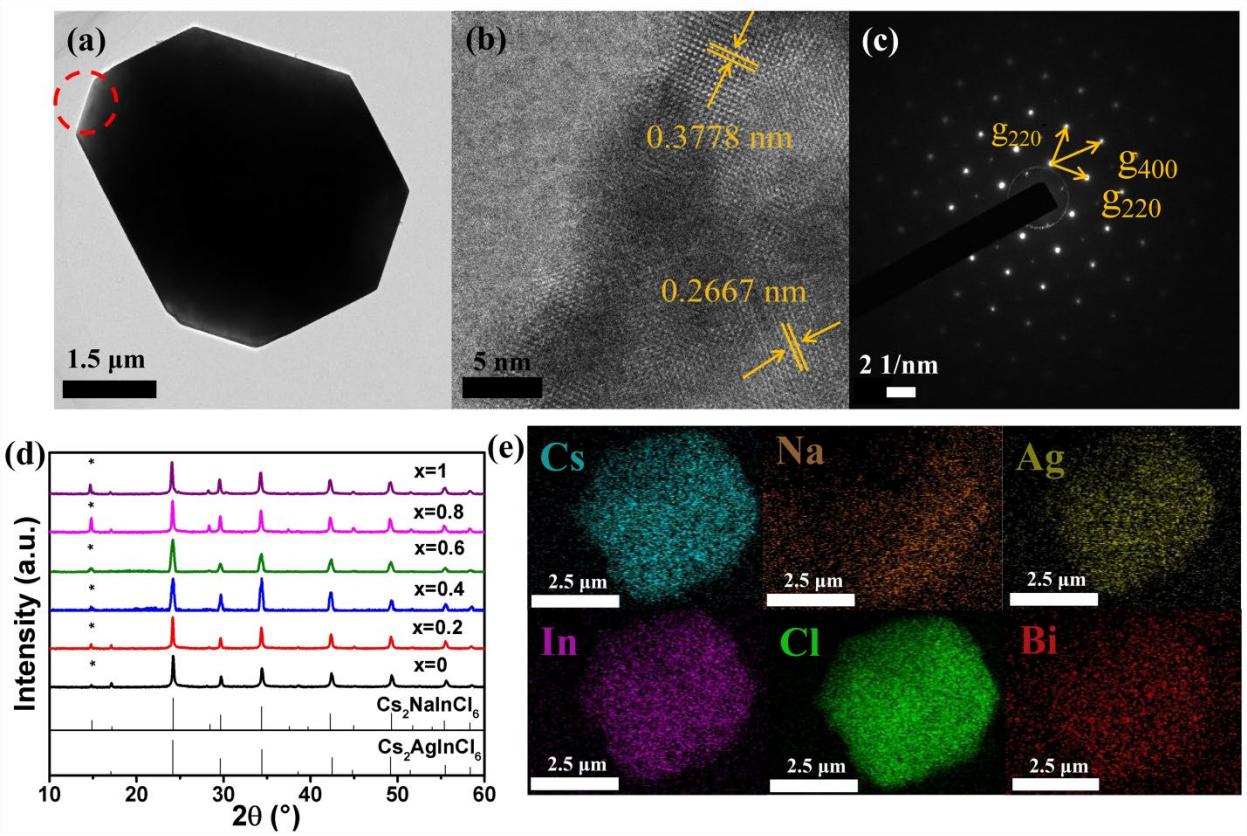

Figure 2. (a) TEM images and (b) high-resolution TEM image for the representative $Cs_2Na_{0.4}Ag_{0.6}InCl_6$: Bi DP-MCs. and (c) A low dose SAED pattern from the red-circled region in Figure 2a. (d) XRD patterns of $Cs_2Na_xAg_{1-x}InCl_6$: Bi MCs (x=0, 0.2, 0.4, 0.6, 0.8, 1) together with the reference pattern of $Cs_2AgInCl_6$ and $Cs_2AgInCl_6$. (e) EDS elemental mapping of $Cs_2Ag_{0.4}Na_{0.6}InCl_6$: Bi DP-MCs.

To further confirm the valence of the elements in the mixed halide compound, the XPS analysis of DP-MCs was conducted. The XPS spectrum shows several characteristic peaks attributable to Cs, Na, Ag, In and Cl elements (**Figure 3a**). The dopant concentrations of Bi^{3+} are too low to be detected by XPS. The positions of the observed peaks are consistent with the expected oxidation states (Cs^+, Na^+, Ag^+, In^{3+}, and Cl^-) for the corresponding metal chlorides.[26] The high-resolution XPS results are illustrated in **Figures 3b-f**. As for Cs 3d spectrum, two peaks appear at 723.8 and

737.8 eV, which could be associated with Cs $3d_{5/2}$ and Cs $3d_{3/2}$, respectively. The In 3d spectra display two peaks at 445.4 and 453.0 eV in DP-MCs, corresponding to the In $3d_{5/2}$ and In $3d_{3/2}$, respectively. The Ag 3d spectra also show two peaks located at 368.0 and 374.0 eV, which can be assigned to Ag $3d_{5/2}$ and Ag $3d_{3/2}$, respectively. The Cl 2p and Na 1s band demonstrated a single peak located at the binding energy of about 199.2 eV and 1072.1 eV, which can be associated to Cl $2p_{3/2}$ and Na $3s_{1/2}$, respectively. This confirms that Na^+ is successfully introduced by replacing Ag^+ in $Cs_2AgInCl_6$ DP lattice.[27]

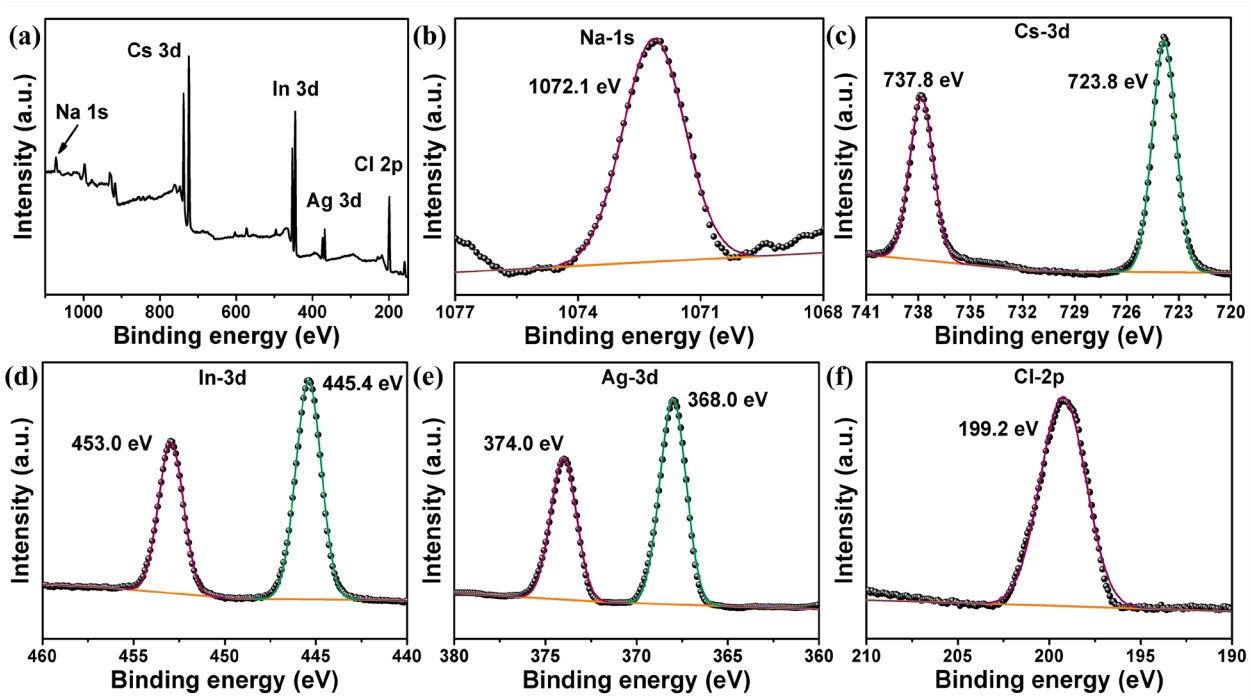

Figure 3. (a) Full XPS spectra and the typical energy regions for (b) Na 1s, (c) Cs 3d, (d) In 3d, (e) Ag 3d and (f) Cl 2p of $Cs_2Ag_{0.4}Na_{0.6}InCl_6$: Bi DP-MCs

Raman spectra illustrated in **Figure S4a** (**Supporting Information**) provide a clear view of the structure information for the DP-MCs. Three peaks are observed and located at 141.9, 170.1, and 301 cm^{-1}, corresponding to the T_{2g}, E_g and A_{1g} vibrations, respectively. Each peak is derived from the mixed vibration of three octahedra: $AgCl_6$, $InCl_6$ and $NaCl_6$. Doping with Bi introduces $BiCl_6$

octahedra into the DP-MCs, giving two additional vibration peaks to the Raman spectra as demonstrated in **Figure S4b** (**Supporting Information**). One peak is T_{2g}, another is E_g, located at 110.4 cm^{-1} and 253.1 cm^{-1}, respectively. Since Ag is substituted by Na, $InCl_6$, $AgCl_6$, and $NaCl_6$ octahedra are working together to maintain the cubic structure symmetry of $Cs_2Na_xAg_{1-x}InCl_6$: Bi DP-MCs. However, the appearance of $NaCl_6$ octahedron still had some effect on Raman vibrational modes by creating some structure distortion. According to the literature, all three octahedra could associate with the A_{1g} mode.[28] To gain more insight into influence of octahedra on Raman vibration modes, the B-Cl (B = Na, Ag, In) bond lengths of the $Cs_2Na_xAg_{1-x}InCl_6$: Bi DP were calculated using the geometrically optimized model in the DS-PAW program. For $Cs_2AgInCl_6$, the bond lengths of Ag-Cl and In-Cl are 2.77 Å and 2.57 Å, respectively. Whereas in $Cs_2NaInCl_6$, the bond lengths of Na-Cl and In-Cl are 2.82 Å and 2.56 Å. The Na-Cl bond has a larger length compared to other B-Cl (B = In, Ag) bonds and vibrates more violently under the influence of external energy, indicating that the strong $NaCl_6$ octahedral vibrations are mainly responsible for the Raman active peaks.

The PL, PL excitation and absorption spectra of $Cs_2Na_{0.4}Ag_{0.6}InCl_6$: Bi DP-MCs are shown in **Figure 4a**. With the FWHM of 216 nm, a broad-band emission is achieved in the DP-MCs under 385 nm excitation. Notably, the absorption peak at around 382 nm can be assigned to the electron transition between valence and conduction bands of the $Cs_2AgInCl_6$ host. Tauc plot, calculated from the corresponding absorption spectrum of $Cs_2AgInCl_6$ DP-MCs demonstrated a direct bandgap of 3.05 eV (**Figure 4b)**. The PLQYs for the $Cs_2Na_xAg_{1-x}InCl_6$: Bi DP-MCs are tabulated in **Table S3** (**Supporting Information**). The poor PLQYs of $Cs_2AgInCl_6$ and $Cs_2NaInCl_6$ DP-MCs can be explained by the parity-forbidden transition of the electronic absorption from valence band maximum to conduction band minimum.[29-31] Therefore, breaking the parity-forbidden

transition becomes a key step to improve the PLQYs. After Na^+ introduction, the PLQY of $Cs_2Na_{0.4}Ag_{0.6}InCl_6$: Bi DP-MCs increased up to 73.3%. Given that Na^+ owns a different electronic configuration than Ag^+, it is believed that the parity-forbidden transition was successfully broken by incorporating Na^+ into the lattice.[32] Meanwhile, the introduction of trace amount Bi^{3+} can improve crystal perfection and facilitate exciton localization,[33-35] and works together with Na^+ incorporation to improve PLQYs of $Cs_2Na_xAg_{1-x}InCl_6$: Bi DP-MCs. Compared to the absorption spectrum of $Cs_2AgInCl_6$: Bi, an absorption band around 385 nm, which is due to the excitonic absorption, emerged in $Cs_2Na_{0.4}Ag_{0.6}InCl_6$: Bi DP-MCs (**Figure S5**, **Supporting Information**). A similar phenomenon was already reported.[16, 36] The PL decay curve of $Cs_2Na_{0.4}Ag_{0.6}InCl_6$: Bi DP-MCs was also studied. As shown in **Figure 4c**, by fitting the PL decay curve with the biexponential equation,[37] the calculated average lifetime is 4.89 μs for $Cs_2Na_{0.4}Ag_{0.6}InCl_6$: Bi DP-MCs. It is found that the lifetimes of samples are less affected by the increasing Na/Ag ratio (**Table S3, Supporting Information**). Therefore, we have selected the representative $Cs_2Na_{0.4}Ag_{0.6}InCl_6$: Bi DP-MC with the highest PLQY for more detailed discussion.

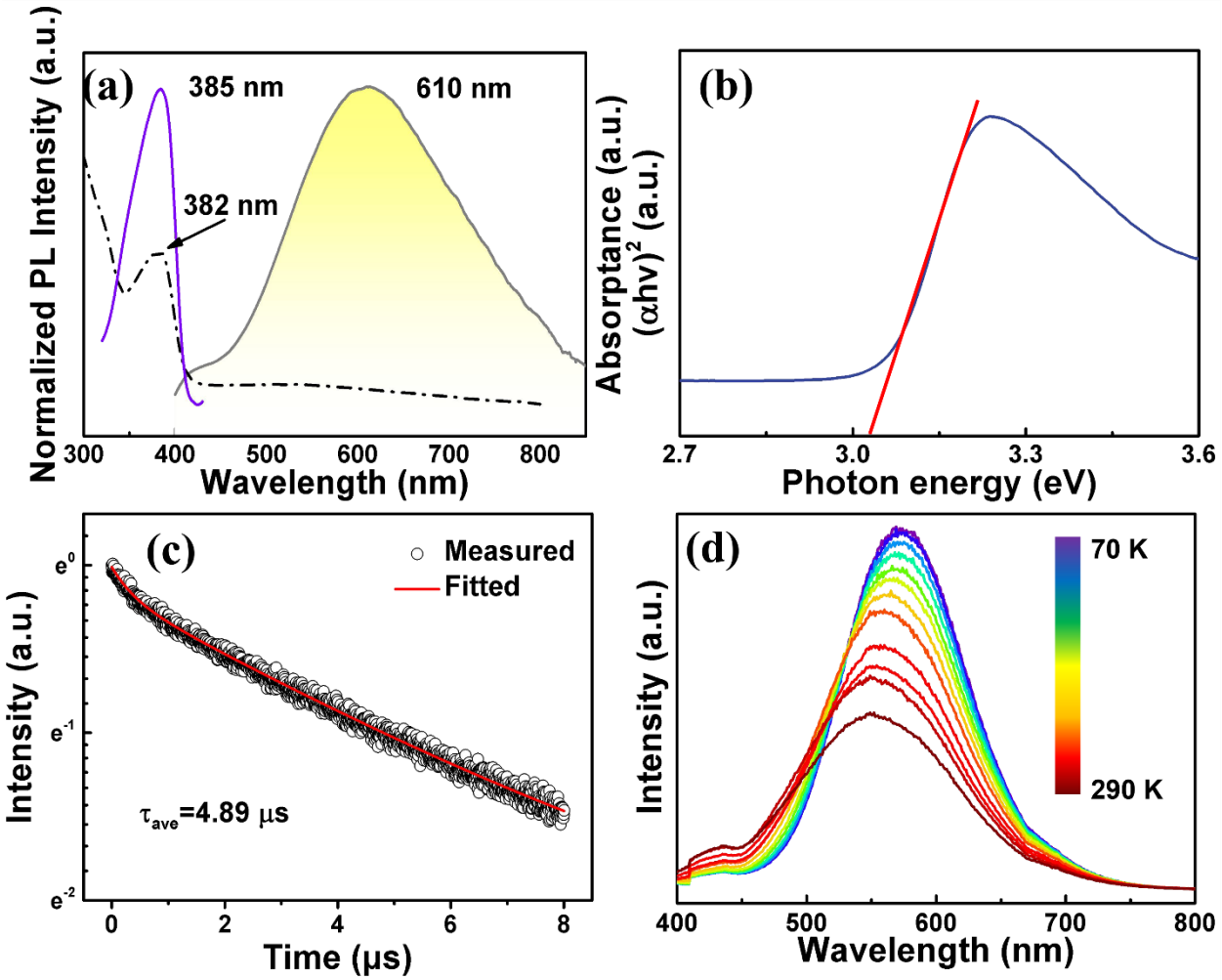

Figure 4. (a) Normalized PL excitation (purple line), absorption (dash line) and emission (grey line) spectra, (b) Tauc plot, (c) PL lifetime, and (d) temperature-dependent emission spectra in the range of 70-290 K (λ=365 nm) of $Cs_2Na_{0.4}Ag_{0.6}InCl_6$: Bi DP-MCs, respectively.

It is generally believed that as the temperature increases, phonons are more likely to couple with excitons, causing non-radiative recombination and leading to a decrease in PL intensity. This is consistent with the results of temperature-dependent PL spectra of the $Cs_2Na_xAg_{1-x}InCl_6$: Bi (x = 0.4, 0.7, and 0.9, in mol %) DP-MCs (**Figure 4d** and **Figure S6**, **Supporting Information**). 48.9%, 42.8% and 76.4% of the initial PL intensity at 70 K were retained at the temperature of 290 K for $Cs_2Na_{0.4}Ag_{0.6}InCl_6$, $Cs_2Na_{0.7}Ag_{0.3}InCl_6$, and $Cs_2Na_{0.9}Ag_{0.1}InCl_6$ DP-MCs, respectively. By using

equation (1) based on the phonon broadening model,[38] the temperature dependence of FWHM can be fitted with Boltzmann distribution.

$$FWHM = 2.36\sqrt{S}\hbar\omega_{\text{phonon}}\sqrt{\coth\left(\frac{\hbar\omega_{\text{phonon}}}{2k_{\text{B}}T}\right)} \quad (1)$$

where Huang-Rhys factor (S) reflects how strongly electrons are coupled to phonons, k_{B} is the Boltzmann constant ($k_{\text{B}} = 8.629 \times 10^{-5}$ eV/K), $\hbar\omega_{\text{phonon}}$ is the phonon frequency and T is the Kelvin temperature. By fitting the Equation (1), the phonon frequency $\hbar\omega$ is about 29.62 meV, 29.04 meV and 28.56 meV for $Cs_2Na_{0.4}Ag_{0.6}InCl_6$, $Cs_2Na_{0.7}Ag_{0.3}InCl_6$ and $Cs_2Na_{0.9}Ag_{0.1}InCl_6$ DP-MCs, respectively(**Figure S7**, **Supporting Information**)[28, 39]. The calculated values of S are 23.98, 24.99 and 26.39 for $Cs_2Na_{0.4}Ag_{0.6}InCl_6$, $Cs_2Na_{0.7}Ag_{0.3}InCl_6$ and $Cs_2Na_{0.9}Ag_{0.1}InCl_6$ DP-MCs, respectively, indicating that all three DP-MCs have an efficient STE emission. Notably, the value of S could reflect the STEs emission intensity, as the value of S decreases, the intensity of the phonon emission decreases, and the PL intensity increases. Therefore, the value of S may become a quality factor for evaluating the white emission from STE. The $Cs_2Na_{0.4}Ag_{0.6}InCl_6$: Bi DP-MCs have a broadband emission and small S value, indicating that this STE emission is likely to be caused by a strong Jahn-Teller distortion of the $AgCl_6$ octahedra. After Na^+ introduction, the newly formed $NaCl_6$ octahedra act as a barrier to limit the spatial distribution of STE, thereby breaking the parity-forbidden transition and increasing probability of radiative recombination.

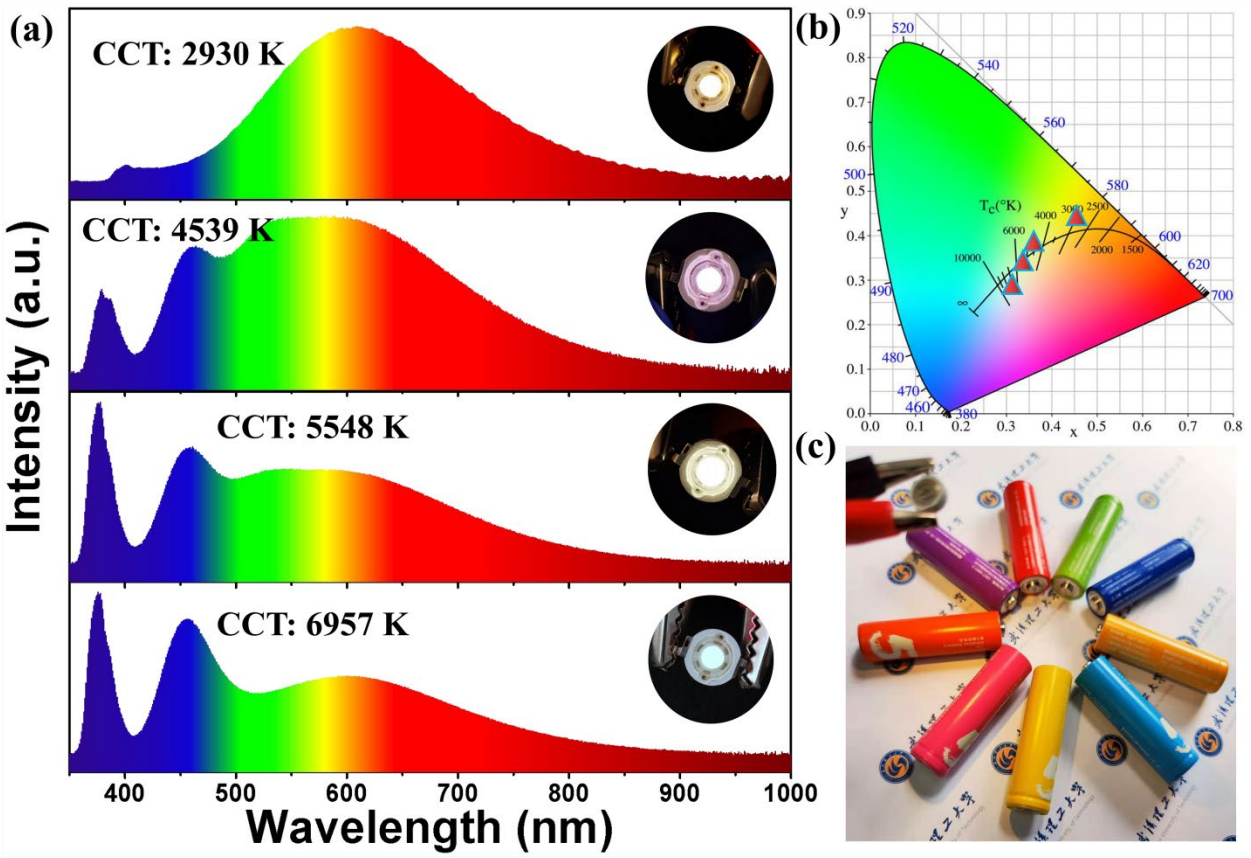

Figure 5. (a) Typical EL spectra of WLEDs under 100 mA with different CCT (Insets are the images of WLEDs), (b) CIE color coordinates of corresponding WLEDs. (c) A photo of an LED with an ultra-high CRI of 97.1.

Along with cost-effective and large-scale synthesis, it is expected that these DP-MCs are promising for fabricating high-performance WLEDs. For this purpose, $Cs_2Na_{0.4}Ag_{0.6}InCl_6$: Bi DP-MCs were mixed with commercial blue and green phosphors and coated on a 365 nm UV-LED to fabricate WLEDs. As shown in **Figure 5a, Figure 5b** and **Table S4** (**Supporting Information**), four WLEDs, with CCT from warm white (2930 K) to cold white (6957 K), the CIE color coordinate from (0.461, 0.443) to (0.313, 0.287), and CRI from 84.8 to ultra-high 97.1 were successfully prepared by adjusting the mass ratio of the three phosphors. The specific ratios of the three phosphors are shown in **Table S4** (**Supporting Information**). **Figure 5c** shows the

photographs of the as-fabricated WLED which has ultra-high CRI of 97.1 emits bright pure white light that features CIE color coordinates of (0.331, 0.340). As shown in **Figure S8** (**Supporting Information**), the fluorescence intensity remained almost constant at different currents while CCT, CRI and CIE color coordinates are also very stable. The above results combined with the good light illumination stability (**Figure S9**, **Supporting Information**) of the $Cs_2Na_{0.4}Ag_{0.6}InCl_6$: Bi DP-MCs phosphors indicate that these lead-free inorganic perovskites phosphors are very promising for WLEDs

Conclusions

A facile solvent-free melting-crystallization synthesis technique was invented to produce $Cs_2Na_xAg_{1-x}InCl_6$: Bi DP-MCs phosphors, which can be mass-produced easily. The formation energy shows that the crystal can be easily formed in a closed vacuum environment. High-quality $Cs_2Na_xAg_{1-x}InCl_6$: Bi DP-MCs with a broadband emission from 400 to 850 nm were successfully prepared. The great increase in PLQYs means the parity-forbidden transition of $Cs_2AgInCl_6$ was successfully broken by introducing Na^+ into the lattice. The $Cs_2Na_{0.4}Ag_{0.6}InCl_6$: Bi that has the highest PLQY of 73.3% has been tested as phosphor for lighting WLEDs. The WLEDs with CCT from warm white (2930 K) to cold white (6957 K), the CIE color coordinate from (0.461, 0.443) to (0.313, 0.287), and CRI from 84.8 to ultra-high 97.1 were successfully prepared by adjusting the mass ratio of this perovskite phosphor, the blue ($BaMgAl_{10}O_{17}$: Eu) and green ($(Sr, Ba)_2SiO_4$: Eu) phosphors. This work has demonstrated an interesting way for developing low-cost, environment-friendly and high-performance inorganic perovskite phosphor for general lighting.

ASSOCIATED CONTENT

Supporting Information

The following files are available free of charge at

Differential thermal analysis (DTA) and thermogravimetric analysis (TGA) data (Figure S1), calculated formation energy data (Table S1), SEM images and EDS data (Figure S2 - S3, Table S2), Raman spectra (Figure S4), optical properties (Figure S5-S9, Table S3-S4) (PDF)

AUTHOR INFORMATION

Corresponding Authors

Yinsheng Xu - State Key Laboratory of Silicate Materials for Architectures, Wuhan University of Technology, Wuhan 430070, China; Email: xuyinsheng@whut.edu.cn

Xianghua Zhang - State Key Laboratory of Silicate Materials for Architectures, Wuhan University of Technology, Wuhan 430070, China; ISCR (Institut Des Sciences Chimiques de Rennes) - UMR 6226, CNRS, Univ Rennes, 35000 Rennes, France; Email: xzhang@univ-rennes1.fr

Authors

Xiaoxi Li - State Key Laboratory of Silicate Materials for Architectures, Wuhan University of Technology, Wuhan 430070, China

Weiwei Li - State Key Laboratory of Advanced Technology for Materials Synthesis and Processing, Wuhan University of Technology, Wuhan 430070, China

Mengling Xia - Wuhan National Laboratory for Optoelectronics (WNLO), Huazhong University of Science and Technology (HUST), Wuhan, Hubei 430074, China.

Chao Liu - State Key Laboratory of Silicate Materials for Architectures, Wuhan University of Technology, Wuhan 430070, China

Neng Li - State Key Laboratory of Silicate Materials for Architectures, Wuhan University of Technology, Wuhan 430070, China

Zuhao Shi - State Key Laboratory of Silicate Materials for Architectures, Wuhan University of Technology, Wuhan 430070, China

Notes

The authors declare no competing financial interest.

ACKNOWLEDGMENT

This work is financially supported by the National Natural Science Foundation of China (61975156), Hubei Natural Science Foundation (2020CFB641), State Key Laboratory of Silicate Materials for Architectures (Wuhan University of Technology, SYSJJ2021-01), Fundamental Research Funds for the Central Universities (203134001). Thanks to Hongzhiwei Technology Co., Ltd. for providing technical support.

References

1. Li, G.; Tian, Y.; Zhao, Y.; Lin, J., Recent progress in luminescence tuning of Ce^{3+} and Eu^{2+}-activated phosphors for pc-WLEDs. *Chem. Soc. Rev.* **2015,** *44* (23), 8688-713.

2. Zhong, J. S.; Gao, H. B.; Yuan, Y. J.; Chen, L. F.; Chen, D. Q.; Ji, Z. G., Eu^{3+}-doped double perovskite-based phosphor-in-glass color converter for high-power warm w-LEDs. *J. Alloys Compd.* **2018,** *735*, 2303-2310.

3. Zhang, F.; Ma, Z.; Shi, Z.; Chen, X.; Wu, D.; Li, X.; Shan, C., Recent advances and opportunities of lead-free perovskite nanocrystal for optoelectronic application. *Energy Mater. Adv.* **2021,** *2021*, 1-38.

4. Majher, J. D.; Gray, M. B.; Strom, T. A.; Woodward, P. M., $Cs_2NaBiCl_6$: Mn^{2+}-A new orange-red halide double perovskite phosphor. *Chem. Mater.* **2019,** *31* (5), 1738-1744.

5. Wei, Y.; Yang, H.; Gao, Z.; Xing, G.; Molokeev, M. S.; Li, G., Bismuth activated full spectral double perovskite luminescence materials by excitation and valence control for future intelligent LED lighting. *Chem. Commun.* **2020,** *56* (64), 9170-9173.

6. Mao, Q.; Shen, B.; Yang, T.; Zhong, J.; Wu, G., A double perovskite-based red-emitting phosphor with robust thermal stability for warm WLEDs. *Ceram. Int.* **2020,** *46* (11), 19328-19334.

7. Noel, N. K.; Stranks, S. D.; Abate, A.; Wehrenfennig, C.; Guarnera, S.; Haghighirad, A.-A.; Sadhanala, A.; Eperon, G. E.; Pathak, S. K.; Johnston, M. B.; Petrozza, A.; Herz, L. M.; Snaith, H. J., Lead-free organic-inorganic tin halide perovskites for photovoltaic applications. *Energy Environ. Sci.* **2014,** *7* (9), 3061-3068.

8. Stoumpos, C. C.; Frazer, L.; Clark, D. J.; Kim, Y. S.; Rhim, S. H.; Freeman, A. J.; Ketterson, J. B.; Jang, J. I.; Kanatzidis, M. G., Hybrid germanium iodide perovskite

semiconductors: active lone pairs, structural distortions, direct and indirect energy gaps, and strong nonlinear optical properties. *J. Am. Chem. Soc.* **2015,** *137* (21), 6804-6819.

9. Liao, Q.; Meng, Q.; Jing, L.; Pang, J.; Pang, Q.; Zhang, J. Z., Highly emissive and stable $Cs_2AgInCl_6$ double perovskite nanocrystals by Bi^{3+} doping and potassium bromide surface passivation. *J. Phys. Chem. C* **2021,** *125* (33), 18372-18379.

10. Slavney, A. H.; Hu, T.; Lindenberg, A. M.; Karunadasa, H. I., A bismuth-halide double perovskite with long carrier recombination lifetime for photovoltaic applications. *J. Am. Chem. Soc.* **2016,** *138* (7), 2138-2141.

11. Manna, D.; Das, T. K.; Yella, A., Tunable and stable white light emission in Bi^{3+}-alloyed $Cs_2AgInCl_6$ double perovskite nanocrystals. *Chem. Mater.* **2019,** *31* (24), 10063-10070.

12. Ma, Z.; Shi, Z.; Yang, D.; Li, Y.; Zhang, F.; Wang, L.; Chen, X.; Wu, D.; Tian, Y.; Zhang, Y.; Zhang, L.; Li, X.; Shan, C., High color-rendering index and stable white light-emitting diodes by assembling two broadband emissive self-trapped excitons. *Adv. Mater.* **2021,** *33* (2), e2001367.

13. Volonakis, G.; Haghighirad, A. A.; Milot, R. L.; Sio, W. H.; Filip, M. R.; Wenger, B.; Johnston, M. B.; Herz, L. M.; Snaith, H. J.; Giustino, F., $Cs_2InAgCl_6$: A new lead-free halide double perovskite with direct band gap. *J. Phys. Chem. Lett.* **2017,** *8* (4), 772-778.

14. Wang, L.; Shi, Z.; Ma, Z.; Yang, D.; Zhang, F.; Ji, X.; Wang, M.; Chen, X.; Na, G.; Chen, S.; Wu, D.; Zhang, Y.; Li, X.; Zhang, L.; Shan, C., Colloidal synthesis of ternary copper halide nanocrystals for high-efficiency deep-blue light-emitting diodes with a half-lifetime above 100 h. *Nano Lett.* **2020,** *20* (5), 3568-3576.

15. Liu, Y.; Rong, X.; Li, M.; Molokeev, M. S.; Zhao, J.; Xia, Z., Incorporating rare-earth terbium(III) ions into $Cs_2AgInCl_6$:Bi nanocrystals toward tunable photoluminescence. *Angew. Chem. Int. Ed.* **2020,** *59* (28), 11634-11640.

16. Luo, J.; Wang, X.; Li, S.; Liu, J.; Guo, Y.; Niu, G.; Yao, L.; Fu, Y.; Gao, L.; Dong, Q.; Zhao, C.; Leng, M.; Ma, F.; Liang, W.; Wang, L.; Jin, S.; Han, J.; Zhang, L.; Etheridge, J.; Wang, J.; Yan, Y.; Sargent, E. H.; Tang, J., Efficient and stable emission of warm-white light from lead-free halide double perovskites. *Nature* **2018,** *563* (7732), 541-545.

17. Liu, Y.; Jing, Y.; Zhao, J.; Liu, Q.; Xia, Z., Design optimization of lead-free perovskite $Cs_2AgInCl_6$:Bi nanocrystals with 11.4% photoluminescence quantum yield. *Chem. Mater.* **2019,** *31* (9), 3333-3339.

18. Zhao, F.; Song, Z.; Zhao, J.; Liu, Q., Double perovskite $Cs_2AgInCl_6$: Cr^{3+}: broadband and near-infrared luminescent materials. *Inorg. Chem. Front.* **2019,** *6* (12), 3621-3628.

19. Blöchl, P. E., Projector augmented-wave method. *Phys. rev. B* **1994,** *50* (24), 17953.

20. Li, S.; Shi, Z.; Zhang, F.; Wang, L.; Ma, Z.; Wu, D.; Yang, D.; Chen, X.; Tian, Y.; Zhang, Y.; Shan, C.; Li, X., Ultrastable lead-free double perovskite warm-white light-emitting devices with a lifetime above 1000 hours. *ACS Appl. Mater. Inter.* **2020,** *12* (41), 46330-46339.

21. Zheng, W.; Sun, R.; Liu, Y.; Wang, X.; Liu, N.; Ji, Y.; Wang, L.; Liu, H.; Zhang, Y., Excitation management of lead-free perovskite nanocrystals through doping. *ACS Appl. Mater. Inter.* **2021,** *13* (5), 6404-6410.

22. Wang, C. Y.; Liang, P.; Xie, R. J.; Yao, Y.; Liu, P.; Yang, Y.; Hu, J.; Shao, L.; Sun, X. W.; Kang, F.; Wei, G., Highly efficient lead-free Bi,Ce-codoped $Cs_2Ag_{0.4}Na_{0.6}InCl_6$ double perovskites for white light-emitting diodes. *Chem. Mater.* **2020,** *32* (18), 7814-7821.

23. Zhou, J.; Xia, Z.; Molokeev, M. S.; Zhang, X.; Peng, D.; Liu, Q., Composition design, optical gap and stability investigations of lead-free halide double perovskite $Cs_2AgInCl_6$. *J. Mater. Chem. A* **2017,** *5* (29), 15031-15037.

24. Locardi, F.; Cirignano, M.; Baranov, D.; Dang, Z.; Prato, M.; Drago, F.; Ferretti, M.; Pinchetti, V.; Fanciulli, M.; Brovelli, S.; De Trizio, L.; Manna, L., Colloidal synthesis of double perovskite $Cs_2AgInCl_6$ and Mn-doped $Cs_2AgInCl_6$ nanocrystals. *J. Am. Chem. Soc.* **2018,** *140* (40), 12989-12995.

25. Luo, J.; Li, S.; Wu, H.; Zhou, Y.; Li, Y.; Liu, J.; Li, J.; Li, K.; Yi, F.; Niu, G.; Tang, J., $Cs_2AgInCl_6$ double perovskite single crystals: parity forbidden transitions and their application for sensitive and fast UV photodetectors. *ACS Photonics* **2017,** *5* (2), 398-405.

26. Nath, B.; Pradhan, B.; Panda, S. K., Optical tunability of lead free double perovskite $Cs_2AgInCl_6$ via composition variation. *New J. Chem.* **2020,** *44* (43), 18656-18661.

27. Locardi, F.; Sartori, E.; Buha, J.; Zito, J.; Prato, M.; Pinchetti, V.; Zaffalon, M. L.; Ferretti, M.; Brovelli, S.; Infante, I.; De Trizio, L.; Manna, L., Emissive Bi-doped double perovskite $Cs_2Ag_{1-x}Na_xInCl_6$ nanocrystals. *ACS Energy Lett.* **2019,** *4* (8), 1976-1982.

28. Siddique, H.; Xu, Z.; Li, X.; Saeed, S.; Liang, W.; Wang, X.; Gao, C.; Dai, R.; Wang, Z.; Zhang, Z., Anomalous octahedron distortion of Bi-alloyed $Cs_2AgInCl_6$ crystal via XRD, Raman, Huang-Rhys factor, and photoluminescence. *J. Phys. Chem. Lett.* **2020,** *11* (22), 9572-9578.

29. Gong, X. K.; Zhang, X. S.; Li, L.; Xu, J. P.; Ding, R. K.; Yin, H.; Zhang, Z. W.; Li, Q.; Liu, L., Blue-light-excited narrowing red photoluminescence in lead-free double perovskite $Cs_{2-x}K_xAg_{0.6}Na_{0.4}In_{0.8}Bi_{0.2}Cl_{6-x}Br_x$ with cryogenic effects. *Inorg. Chem. Front.* **2022**.

30. Li, S.; Luo, J.; Liu, J.; Tang, J., Self-trapped excitons in all-inorganic halide perovskites: fundamentals, status, and potential applications. *J. phys. chem. lett.* **2019,** *10* (8), 1999-2007.

31. Ma, Z.; Li, Q.; Luo, J.; Li, S.; Sui, L.; Zhao, D.; Yuan, K.; Xiao, G.; Tang, J.; Quan, Z., Pressure-driven reverse intersystem crossing: new path toward bright deep-blue emission of lead-free halide double perovskites. *J. Am. Chem. Soc.* **2021,** *143* (37), 15176-15184.

32. Meng, W.; Wang, X.; Xiao, Z.; Wang, J.; Mitzi, D. B.; Yan, Y., Parity-forbidden transitions and their impact on the optical absorption properties of lead-free metal halide perovskites and double perovskites. *J. Phys. Chem. Lett.* **2017,** *8* (13), 2999-3007.

33. Zhang, F.; Zhao, Z.; Chen, B.; Zheng, H.; Huang, L.; Liu, Y.; Wang, Y.; Rogach, A. L., Strongly emissive lead-free 0D $Cs_3Cu_2I_5$ perovskites synthesized by a room temperature solvent evaporation crystallization for down-conversion light-emitting devices and fluorescent inks. *Adv. Opt. Mater.* **2020,** *8* (8), 1901723..

34. Zhou, B.; Liu, Z.; Fang, S.; Zhong, H.; Tian, B.; Wang, Y.; Li, H.; Hu, H.; Shi, Y., Efficient white photoluminescence from self-trapped excitons in Sb^{3+}/Bi^{3+}-codoped $Cs_2NaInCl_6$ double perovskites with tunable dual-emission. *ACS Energy Lett.* **2021,** *6* (9), 3343-3351.

35. Xie, L.; Chen, B.; Zhang, F.; Zhao, Z.; Wang, X.; Shi, L.; Liu, Y.; Huang, L.; Liu, R.; Zou, B., Highly luminescent and stable lead-free cesium copper halide perovskite powders for UV-pumped phosphor-converted light-emitting diodes. *Photonics Research* **2020,** *8* (6), 768-775.

36. Mahor, Y.; Mir, W. J.; Nag, A., Synthesis and near-infrared emission of Yb-doped $Cs_2AgInCl_6$ double perovskite microcrystals and nanocrystals. *J. Phys. Chem. C* **2019,** *123* (25), 15787-15793.

37. Dahl, J. C.; Osowiecki, W. T.; Cai, Y.; Swabeck, J. K.; Bekenstein, Y.; Asta, M.; Chan, E. M.; Alivisatos, A. P., Probing the stability and band gaps of $Cs_2AgInCl_6$ and $Cs_2AgSbCl_6$ lead-free double perovskite nanocrystals. *Chem. Mater.* **2019,** *31* (9), 3134-3143.

38. Tan, Z.; Chu, Y.; Chen, J.; Li, J.; Ji, G.; Niu, G.; Gao, L.; Xiao, Z.; Tang, J., Lead-free perovskite variant solid solutions $Cs_2Sn_{1-x}Te_xCl_6$: bright luminescence and high anti-water stability. *Adv. Mater.* **2020,** *32* (32), 2002443.

39. Manna, D.; Kangsabanik, J.; Das, T. K.; Das, D.; Alam, A.; Yella, A., Lattice dynamics and electron-phonon coupling in lead-free $Cs_2AgIn_{1-x}Bi_xCl_6$ double perovskite nanocrystals. *J. Phys. Chem. Lett.* **2020,** *11* (6), 2113-2120.

Table of Contents.

A novel solvent-free melting-crystallization synthesis of bright warm white emissive Lead-free double perovskites microcrystals (DP-MCs) with quantum yields (QYs) up to 73.3% is demonstrated.